Phytotoxic ozone dose and the role of environmental factors in ozone uptake of dwarf mountain pine

Svetlana Bičárová[1], Zuzana Sitková[2], Hana Pavlendová[2], Peter Fleischer jr.[3], Peter Fleischer sr.[3], and Andrzej Bytnerowicz[4]

[1]Institute of Earth Science of the Slovak Academy of Sciences, Stará Lesná, 059 60 Tatranská Lomnica, Slovakia
[2]National Forest Centre–Forest Research Institute Zvolen, T. G. Masaryka 22, 960 92 Zvolen, Slovakia
[3]Technical University in Zvolen, T. G. Masaryka 24, 960 92 Zvolen, Slovakia
[4]USDA Forest Service, Pacific Southwest Research Station, 4955 Canyon Crest Drive, Riverside, CA 92507, USA

Correspondence to: Svetlana Bičárová (bicarova@ta3.sk)

Abstract. Montane forests are exposed to high ambient ozone (O_3) concentrations that may adversely affect physiological processes in internal cells when O_3 molecules enter the plants through the stomata. This study addresses the model results of Phytotoxic Ozone Dose (POD) based on estimation of stomatal O_3 flux to dwarf mountain pine (*P. mugo*) in the Slovak part of the High Tatra Mountains. POD ozone metrics were calculated by deposition model DO_3SE using O_3 concentration and meteorological data measured in three different altitudinal zones during year of 2016. In addition, key model parameter i.e. maximal stomatal conductance (G_{max}) derived from gasometric field measurement in local conditions was included to model data processing. Field measurement also confirmed appropriate performance of DO_3SE model for stomatal conductance (G_{sto}). Site-specific stomatal conductance response model coincided well with average values estimated by DO_3SE, but differed in temporal G_{sto} distribution. We found moderate limitation of O_3 uptake due to environmental factors (f_{ENVI}) if we considered real air humidity, solar radiation, and soil water conditions. It appears that parameter G_{max} is more relevant for year round POD than f_{ENVI}, although model simulation for optimal air temperature suggests further increase of stomatal O_3 uptake as response of global warming. We also identified visible O_3 injury on the needles of *P. mugo*, more evident for two year old than the younger needles. Presented results indicate high level of POD and O_3 uptake of *P. mugo* in the High Tatra Mountains environment that correspond with observation of O_3 induced visual symptoms.

1 Introduction

Surface ozone (O_3) is one of the most common air pollutants according to on a recent review of the accumulated scientific evidence (WHO, 2006; EPA, 2014; EEA, 2016; UNECE, 2016). During recent decades, trends in mean O_3 concentrations have varied by regions (Cooper et al., 2014) nevertheless did not appear to be well associated with some exposure metrics applicable for assessing human health or vegetation effects (Lefohn et al., 2017). A variety of O_3 metrics are used in the risk assessment for forest trees. Initially developed (or original) exposure standards (AOT40) based only on measured O_3 concentration does not take into account environmental factors and physiological conditions affecting responses of vegetation. Therefore in late

1990s a discussion on developing new, flux-based critical levels, started. New approaches focus on the principles of O_3 transport from atmosphere to the plant interior through the stomata, and control of O_3 uptake by leaves *via* environmental factors (Fuhrer et al., 1997; Massman et al., 2000; Grünhage et al., 2001; Ashmore et al., 2004; Musselman et al., 2006; Karlsson et al., 2007; Matyssek et al., 2007). A stomatal conductance-based model was developed to estimate O_3 uptake for a number of the most widespread tree species (Emberson et al., 2000; Emberson et al., 2007; Büker et al., 2012). The new flux-based critical levels revised by the LRTAP Convention (CLRTAP, 2015; Mills et al., 2011) were named as the Phytotoxic Ozone Dose (POD_Y), i.e., the accumulated stomatal O_3 flux above a threshold (Y) flux. There is strong support among biologists for the use of the threshold O_3 flux that includes the detoxification capacity of the trees (Karlsson et al., 2007; Büker et al., 2015). Expert judgement was used to set Y=1 nmol m^{-2} PLA s^{-1} (PLA is the projected leaf area) based on observation of O_3 sensitivity under controlled conditions (Dizengremel et al., 2013). The most recent studies such as Feng et al. (2017) revealed that to move from a leaf area-based to a leaf mass-based stomatal ozone flux index POD_X (X represents the mass-based flux threshold) simplifies large-scale impact assessment for trees since it potentially allows for one common dose–response relationship for all tree species. On the other hand, De Marco et al. (2015) recommend applying POD_Y without threshold limitation (Y=0) i.e., POD_0 rather than POD_1. It is based on the fact that any O_3 molecule entering into the leaf may induce a metabolic response (Musselman et al., 2006). Various studies have provided information on how O_3 interacts with the plant at the cellular level (Bussotti et al., 2011; Gottardini et al., 2014; Braun et al., 2014; Mills et al., 2016). In addition, the physiological consequences of the O_3 induced effects may impair resistance of trees to the abiotic (frost, drought) and biotic (nutrient deficiencies, pathogens, bark beetle) stress factors (Vollenweider and Günthardt-Goerg, 2006). In recent decades, also the forests in the studied High Tatra Mountains have been repeatedly damaged by the massive windstorms and consecutive bark beetle (*Ips typographus)* outbreaks and weakened by accompanying abiotic factors such as elevated temperature (Mezei et al., 2017) or long-range transport of air pollutants (Bytnerowicz et al., 2004).

The major challenge in the development of O_3 standards is their validation against biologically based field data (Paoletti and Manning, 2007). Recent epidemiological studies show better correlation between POD_0 and visible foliar O_3 injury than AOT40 (Sicard et al., 2016). The most sensitive conifers are *Pinus* species in the Mediterranean region (Dalstein and Vas, 2005), however different visible O_3 injury response may be expected under specific local conditions (Coulston et al., 2003; Nunn et al., 2007; Braun et al., 2014). Based on large literature evidence, mountain forest in the Carpathians (Bytnerowicz et al., 2004; Hůnová et al., 2010; Zapletal et al., 2012; Bičárová et al., 2016), and in the Alps (Smidt and Herman, 2004; Sicard et al., 2011) are exposed to high O_3 concentrations. Ozone damage rates increase with altitude in response to increasing O_3 mixing ratios and O_3 uptake due to favourable microclimatic conditions (Díaz-de-Quijano et al., 2009). However there is still lack of empirical data concerning vulnerable mountain tree species.

The objectives of this study were: (i) to map POD_Y ozone metrics (POD_1, POD_0) for year round growing season 2016; (ii) to appraise the role of environmental factors in O_3 uptakes; and (iii) to analyse the relation between model results of POD_Y and

field observation of visual O_3 injury for dwarf mountain pine (*Pinus mugo* Turra). To achieve these goals we focused on mountain region of the High Tatra Mountains (SK–HT) in the Western Carpathians.

2 Study area

The study area (Fig. 1**)** covers montane forest sites in SK–HT region situated in the highest mountain range of the Western Carpathians. The elevation in this region rises from foothills at 800 m a.s.l. to the highest peak at 2,655 m a.s.l.. Climate is mostly cold and humid. According to standard reference climate period (1961–1990), mean annual air temperature ranges from 5.3 °C at foothills to –3.8 °C in zone above 2,600 m a.s.l. Mean annual precipitation varies from 760 to 2,000 mm. In the warmer half of year (Apr–Sep) precipitation reaches nearly 65 % of annual sum with culmination in June or July. The natural coniferous forest dominated by Norway spruce spreads up to 1,600 m a.s.l. Subalpine zone (up to 1,800 m a.s.l.) creates a continuous belt and is almost completely covered by dwarf mountain pine. In recent decades spruce forest has been seriously weakened by long-distance pollution (Bytnerowicz et al., 2004), heavy windstorms and bark beetle outbreaks which reduced forest cover by 50 % (Fleischer et al., 2017). Such a drastic reduction of forest area increased the role of dwarf mountain pine for landscape ecological stability in the High Tatra Mountains region as it still remains relatively undisturbed species neither by abiotic nor biotic factors. Dwarf mountain pine has been successfully planted outside its natural high mountain biotopes for provision of various ecosystem services, e,g. slope and water regime stabilisation, greening projects etc. To map phytotoxic O_3 doses and to estimate further functioning of dwarf pine under changing conditions we have established three study sites distributed in different altitudes: A–foothills, B–submontane zone, C–subalpine zone and different aspects: south (sites A, C) and north (site B). To illustrate variability of O_3 concentration in the lower troposphere we included into study area the additional ground-based O_3 measurement site (D) situated at the peak of Lomnický štít (Table 1, Fig. 1).

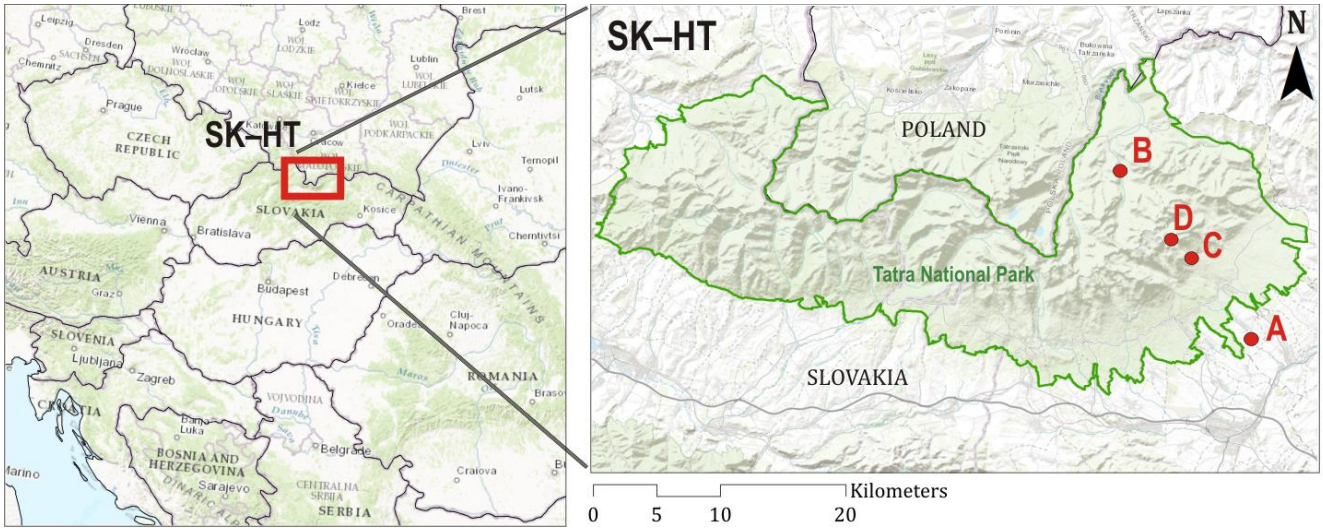

Figure 1. Geographical position of the High Tatra Mts. study area (SK–HT) in the Carpathian mountain range and location of experimental sites in different altitudes; A – Stará Lesná (810 m a.s.l); B – Podmuráň (1,100 m a.s.l.); C – Skalnaté Pleso (1,778 m a.s.l.); D – Lomnický štít (2,635 m a.s.l.).

Table 1. Description of experimental sites (CODE used in relation to Fig. 1). Long-term average of annual air temperature (AT) and precipitation sum (P) is valid for reference climate period of 1961–1990.

CODE Site name	GPS Latitude Longitude	Altitude Zone/Aspect	$AT_{1961–1990}$ [deg C]	$P_{1961–1990}$ [mm]	Soil type Soil texture
A Stará Lesná	49°09'08" N 20°17'19" E	810 m a.s.l. Foothill/South	5.3	759	Haplic Cambisols; Silt loam (medium coarse)
B Podmuráň	49°15'00" N 20°09'25" E	1,100 m a.s.l. Submontane/North	4.0	1,227	Haplic Podzols; Loam (medium)
C Skalnaté Pleso	49°11'21" N 20°14'02" E	1,778 m a.s.l. Subalpine/South	1,7	1,282	Folic Leptosols; Sandy loam (coarse)
D Lomnický štít	49°11'43" N 20°12'54" E	2,635 m a.s.l. Alpine summit	-3.8	1,239	Lithic Leptosols; Hyperskeletic

3 Methods

3.1 Ozone metrics

Stomatal flux based O_3 metrics (POD_Y) were calculated using the multiplicative model DO_3SE (Deposition of Ozone for Stomatal Exchange), (SEI, 2014). An algorithm for model estimation of POD_Y (mmol m^{-2} PLA) incorporates effects of meteorological conditions such as air temperature (f_{temp}), vapour pressure deficit (f_{VPD}), solar radiation or light (f_{light}), furthermore soil water potential (f_{SWP}), plant phenology (f_{phen}) and O_3 concentration (f_{O3}) on the maximum stomatal conductance (G_{max}). In the case of conifer type of trees, the ozone and phenology functions are considered to be constant (f_{O3} =1, f_{phen} =1) due to moderate senescence promoting effect on stomatal conductance. The f_{min} function expresses a fraction of G_{max} and represents the relative minimum stomatal conductance that occurs during daylight hours.

Passage rate of O_3 entering through the stomata expresses the stomatal O_3 conductance G_{sto} (mmol O_3 m^{-2} s^{-1}):

$$G_{sto} = G_{max} * [min(f_{phen}, f_{O_3})] * f_{light} * max\{f_{min}, (f_{temp} * f_{VPD} * f_{SWP})\} = G_{max} * f_{ENVI} \quad (1)$$

Stomatal O_3 flux F_{st} (nmol m^{-2} PLA s^{-1}) is given by:

$$F_{st} = G_{sto} * c(z_1) * \left(\frac{r_c}{(r_b+r_c)}\right) = G_{max} * f_{ENVI} * c(z_1) * \left(\frac{r_c}{(r_b+r_c)}\right) \quad (2)$$

where $c(z_1)$ is concentration of O_3 (nmol m^{-3}) at the top of the canopy measured in the tree height (z_1), r_b and r_c are the quasi laminar resistance and the leaf surface resistance (s m^{-1}), respectively.

Phytotoxic ozone dose POD_Y is sum of hourly values of F_{st} (Eq. 2) over threshold Y=1 (POD_1) or without threshold Y=0 (POD_0) aggregated over the period between start (SGS) and end (EGS) of the growing season. In the case of conifers we can consider year round period from 1st January to 31st December.

$$POD_Y = \sum_{SGS}^{EGS} \lfloor (F_{st} - Y) * (3600/10^6) \rfloor \quad (3)$$

Stomatal flux-based critical levels CLef$_1$ of POD$_1$ was set to value of 9.2 mmol m^{-2} PLA for an acceptable biomass loss of forest trees, especially Norway spruce CLRTAP, 2017). An innovative species-specific CLef of POD$_0$ is proposed to be 19 mmol m^{-2} PLA for forest protection against visible O_3 injury for high O_3 sensitive pine tree species (Sicard et al., 2016). More specific description of the algorithm and derivation of the physical relationships for the final calculation of POD$_Y$ is given in the manual for modelling and mapping of the critical level exceedance (CLRTAP, 2015; Mills et al., 2011). The parameterization of DO$_3$SE model reflects the recommendations in different scientific papers, the generic values are also given in manual ICP Modelling and Mapping (ICP, 2016). In this work, the preset built in version 3.0.5 of DO$_3$SE model (SEI, 2014) with collection of parameters for coniferous forests (CF) was used (Table S1). Maximal stomatal O_3 conductance G_{max} (mmol O_3 m^{-2} PLA s^{-1}) as key parameter of stomatal O_3 flux (Eq. 2) of dwarf mountain pine was obtained according to field experiments (Fig. 2 left). Model requires input files that include measured O_3 concentration and meteorological data, for each experimental site separately.

3.2 Ozone and meteorological data

Measurement of O_3 concentration was provided by active monitors (Horiba–APOA360, Thermo Electron Environmental 49C and 2B Tech Ozone Monitor M106-L) based on the well established technique of UV absorption by O_3 at wavelenght 254 nm. Hourly mean data at three experimental forest stands (A, B, C) were recorded in continuous regime without major gaps during year 2016. Furthermore, O_3 concentrations measured at experimental site Lomnický štít (D) were considered for illustration of O_3 variability in different altitudes varying between 810 and 2,635 m a.s.l. The meteorological variables were continuously monitored at all experimental sites using the measurement system based on PROlog – ultra low power datalogger (Physicus, SK). At all sites the following identical sensors were used for the measurement: the temperature probe with platinum resistance thermometers Pt100 for the air temperature (at 2 m level above the surface); Prove-HumiAir 9 for the relative air humidity; the Pyranometer CMP3 (Kipp and Zonen) for the global solar radiation; the Wind Transmitter Compact (Thies Clima) for wind speed, PressAir sensor for the air pressure, and the Rain Gauge MR3H - Meteoservice(CZ) for the precipitation. Selected meteorological data allow to specify the environmental functions associated with air temperature (Eq. 4), vapour pressure deficit (Eq. 5), irradiance radiation and light (Eq. 6):

$$f_{temp} = max\left\{f_{min}, \left[\left(\frac{AT-T_{min}}{T_{opt}-T_{min}}\right) * \left(\frac{T_{max}-AT}{T_{max}-T_{opt}}\right)\right]^{\left(\frac{T_{max}-T_{opt}}{T_{opt}-T_{min}}\right)}\right\} \quad (4)$$

$$f_{VPD} = min\left\{1, max\left[f_{min}, \left((1-f_{min}) * \left(\frac{VPD_{min}-VPD}{VPD_{min}-VPD_{max}}\right)\right) + f_{min}\right]\right\} \quad (5)$$

$$f_{light} = 1 - EXP\left((-light_a) * PFD\right) \quad (6)$$

where AT is measured air temperature (°C); VPD (kPa) is vapour pressure deficit calculated on base of measurement of air temperature and relative air humidity; PFD represents the photosynthetic photon flux density in units of μmol m^{-2} s^{-1} i.e.

photosynthetically active radiation (PAR) derived from measurement of global solar radiation R (W m^{-2}). These variables are completed by species specific parameters f_{min}, T_{min}, T_{opt}, T_{max}, VPD_{min}, VPD_{max}, $light_a$ listed in Table S1. Functions of f_{temp}, f_{VPD}, and f_{light} are expressed in relative terms (i.e., it takes values between 0 and 1 as a proportion G_{max}).

3.3 Soil water potential

Soil moisture data were obtained by two approaches: field measurements and modelling. Both, real-time and modelled data of soil water potential (SWP) are useful for specification of the f_{SWP} function (Eq. 7).

$$f_{SWP} = min\left\{1, \left\{f_{min}\left((1 - f_{min}) * (SWP_{min} - SWP)/(SWP_{min} - SWP_{max})\right) + f_{min}\right\}\right\} \quad (7)$$

Function of f_{SWP} defines the effect of soil moisture on G_{sto} (Eq. 1) in relative terms similar as the above-mentioned functions (Eq. 4–6). Additional parameters such as f_{min}, SWP_{min}, SWP_{max} are listed in Table S1. Differences between f_{SWP} based on measured and modelled SWP allow to verify the reliability of the soil moisture module included in DO_3SE model. Modelling approach incorporated hydraulic resistance (steady state, SS) to water flow through the plant system (Büker et al., 2012). Field measurement of SWP was carried out at three soil depths (–0.1, –0.2, –0.4 m) and at all experimental sites (except the cliff of Lomnický štít). SWP values we measured using gypsum blocks in the range up to –1.5 MPa (GB2, Delmhorst Instrument, U.S.A.). Data of SWP were stored into the integrated data loggers (MicroLog SP3, EMS Brno, CZ) in 1-hour intervals.

3.4 Maximum level of stomatal ozone conductance

Data on maximum stomatal conductance, or just general response of dwarf mountain pine stomata to environmental factors are rather sparse or even absent in literature. Maximal stomatal conductance (G_{max}, mmol O_3 m^{-2} PLA s^{-1}) is a key parameter (Eq. 1) for calculation of stomatal O_3 flux in DO_3SE model (Eq. 2). Data required for G_{max} estimation provided direct measurement. For this purpose LI-6400 photosynthesis system (Li-Cor, Inc., Lincoln, NE) equipped with a standard Licor 6400-22 Opaque Conifer Chamber and 6400–18 RGB Light Source was used. To capture wide range of climatic conditions we measured the stomatal conductance from June to November at two study sites situated in different elevations: site A (Stará Lesná, 810 m a.s.l.) and site C (Skalnaté Pleso, 1,778 m a.s.l.). During the experiment, inside chamber temperature ranged from 5 to 35 °C, VPD from 0.2 to 3.5 kPa, photosynthetic photon flux density (PPFD) from 0 to 2,500 µmol photons m^{-2} s^{-1}, CO_2 concentration was set to 400 ppm. Before each measurement, gas exchange was permitted to stabilize for approximately 6–10 min. Gas exchange measurements were conducted frequently on attached healthy looking sunlit terminal shoots of lateral branches from middle part of the plant. On average 8–9 measurements under different conditions were recorded per shoot. We considered G_{sto} (mmol O_3 m^{-2} PLA s^{-1}) from G_{sto} (mmol H_2O m^{-2} PLA s^{-1}) using a conversion factor of 0.663 (Massman, 1998) to account for the difference in the molecular diffusivity of water vapour (measured by LI-6400 photosynthesis system) to that of ozone. Values of G_{sto} within the top 5 percent in range between 110 and 160 mmol O_3 m^{-2} PLA s^{-1} were noticed. Maximum stomatal conductance G_{max} was derived as the 95 percentile of all measured data of stomatal conductance for O_3 flux rates

(about 2,700 measurements of G_{sto}) after removal of outliers. Based on this derivation, maximum level of stomatal O_3 conductance for dwarf mountain pine was determined as G_{max}=110 mmol O_3 m^{-2} PLA s^{-1} (Fig. 2 left).

In order to verify performance of stomatal conductance in DO_3SE model for dwarf mountain pine in SK–HT we developed site-specific stomata response function. Stomatal conductance measured at 800 and 1,700 m a.s.l allowed to construct local model covering wide spectrum of environmental conditions (air temperature, leaf temperature, VPD, CO_2 concentration, RH, PAR, air pressure, SWP, soil moisture and temperature). The model was derived by symbolic regression approach using HeuresticLab ver. 3.13 software (Wagner et al., 2014) from 2400 readings of stomatal conductance. Two third of field data (randomly selected 1,600 measurements) were used for model development and one third (800 measurements) for evaluation of model performance. Final simplified and optimized model was as follows:

$$Gsto = \left(\frac{AT*log((c_0*AT+c_1))*c_2}{c_3*VPD}\right) + c_4 \quad (8)$$

with parameters: c_0 = 1.9854, c_1 = - 16.34, c_2 = 0.16571, c_3 = 267.39 and c_4 = 0.01287.

Seasonal variation of stomatal conductance (G_{sto}) was reliably (Pearson's R^2=0.63, mean absolute error MAE=7.7 mmol O_3 m^{-2} s^{-1}, average relative error ARE=10 %) described by two variables (AT– air temperature and VPD – vapour pressure deficit). Measured and modelled (Eq. 8) stomatal conductance data are shown in Fig. 2 (right).

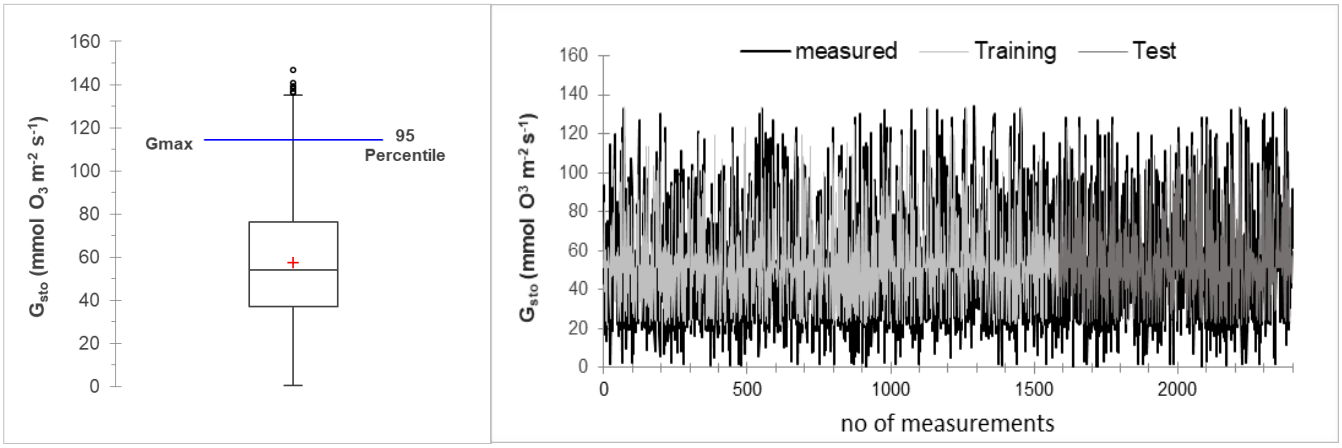

Figure 2. Stomatal conductance (G_{sto}) for dwarf mountain pine in SK–HT: (left) box plot of measured data and derived parameter G_{max}; (right) comparison of G_{sto} measured by Licor6400XT (black) and modelled by site-specific regression function, ligh grey training data and dark grey test data.

3.6 Visible ozone injury

Observation of visible injury symptoms on dwarf mountain pine needles collected in the late autumn 2016 was undertaken in accordance with the methods recommended for analysis of the effects of air pollution on forests (ICP, 2016). We evaluated the branches of dwarf mountain pine sampled from eleven plots situated along altitudinal profile from 800 to 2,000 m a.s.l.. At each plot we selected 5 sample trees exposed to sun. For each tree, 5 branches with at least 30 needles per each needle age class (current year foliage (C), one year old (C+1) and two year old needles (C+2)) were removed from the upper third of the

crown. For each branch, we scored the percentage of total needle surface affected by visible foliar O_3 injury for C, C+1 and C+2. Finally, we calculated a mean percentage of needles surface affected by visible foliar O_3 injury per every plot.

4 Results

4.1 Variability of O_3 concentration and meteorological data

As we expected, the mean annual O_3 concentrations covering year round period of 2016 (Table 2) increased with rising altitudes from 28.7 ppb (A) to 48.5 ppb (D). Therefore, timberline vegetation of the subalpine (C) and alpine zone (D) is high risk to injury effect of O_3 air pollution (Fig. 3a). The monthly mean of O_3 concentration varied between 20 ppb and 40 ppb from the foothill (A) up to submontane (B) zone while in the subalpine (C) and alpine zones were above 40 ppb (D). Monthly O_3 mean culminated in May (Fig. 3b) and achieved values between 36.3 ppb (B) and 59 ppb (D). The diurnal variation of hourly O_3 concentration (Fig. 3c) at lower altitudes (A, B) clearly contrasted with relatively flatling course at higher elevations (C, D). Hourly mean O_3 concentration varied between 20 and 40 ppb for foothills and submontane zone during daytime while at higher altitudes fluctuated near to level of 50 ppb for all hours of day. These high O_3 concentrations occurred in cold a humid climate of subalpine and alpine zone where annual mean air temperature achieved values of 3.0 °C and -3.2 °C, respectively (AT, deg C in Table 2). Annual mean values as well as maxima of vapour pressure deficit (VPD, kPa) suggested air humidity conditions favourable for unlimited stomatal conductance (Table S1) at all plots. Precipitation totals (P, mm) between 1,545 mm and 2,277 mm ensured a sufficient supply of soil water for roots of dwarf mountain pine from the submontane up to alpine zone. Measurement of global solar radiation (R, kW m^{-2}) confirmed the assumption of lower value of total solar irradiance on the north exposure site (B) in comparison with plots situated on southern part of SK–HT.

Table 2. Statistics of hourly O_3 and meteorological data in different altitude zones during the year round period of 2016

Variables	Statistic	A	B	C	D
O_3 concentration	O_3 (ppb)				
	Mean	28.7	29.6	45.9	48.5
	Max	64.0	68.6	81.2	86.0
	Min	2.3	1.7	10.0	15.7
	STD	11.7	13.8	9.1	8.7
Air temperature	AT (°C)				
	Mean	6.5	5.0	3.0	-3.2
	Max	29.9	27.8	23.1	16.6
	Min	-18.9	-20.1	-18.7	-22.5
	STD	8.9	8.2	7.5	7.5
Vapour pressure deficit	VPD (kPa)				
	Mean	0.27	0.17	0.19	0.12
	Max	2.30	1.80	1.56	1.60
	Min	0.02	0.01	0.02	0.00
	STD	0.33	0.24	0.18	0.18
Precipitation	P (mm)				
	Mean	0.08	0.18	0.18	0.39

	Max	37.6	28.6	27.6	71.2
	Sum	727	1,545	1,601	2,277
	STD	0.61	0.91	0.80	0.49
Global solar radiation	R (kW m^{-2})				
	Mean	0.13	0.10	0.12	0.13
	Max	1.03	1.01	1.15	0.97
	Sum	1,133	900	1,068	1,136
	STD	0.22	0.20	0.20	0.20

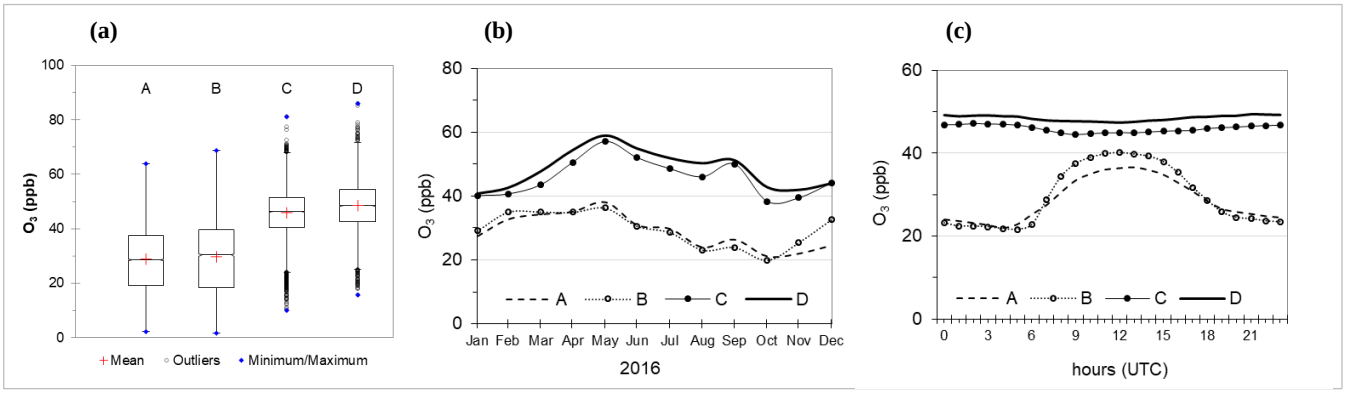

Figure 3. Variability of measured hourly O_3 data: (a) annual means, (b) monthly means, and (c) diurnal variation of O_3 concentration in different altitudes (A, B, C, D) in 2016.

4.2 Response of stomatal conductance to environmental factors

Relation between meteorological factors: f_{temp}, f_{VPD}, f_{light} (Eq. 4–6) derived on base of measured data (Table 2) and stomatal conductance G_{sto} (Eq. 1) is illustrated in Fig. 4. As we have expected, relatively cool and humid mountain climate in SK–HT did not limit G_{sto} due to absence of extremely high air temperatures (>T_{max}) as well as low air humidity (> VPD_{min}). Except frosty days in winter season, air temperatures varied mostly in interval between T_{min} and T_{opt}, Frequency of air temperature higher than T_{opt} decreased from foothills (A) to subalpine zone (C). Similarly, VPD values above VPD_{max} were more frequent on foothills (A) when compared to sites situated in higher elevation (B, C). Solar light conditions characterised by photosynthetically active radiation (PAR) were comparable for southern exposed plots (A, C). Although northern plot (B) received slightly less solar energy (Table 2), values of f_{light} associated with PAR were not substantially different. Upper values of G_{sto} achieved level of 90 mmol O_3 m^{-2} s^{-1} if we considered measurement based parameter G_{max} = 110 mmol O_3 m^{-2} s^{-1} (Fig. 2 left). In case of model based G_{max} = 160 mmol O_3 m^{-2} s^{-1} (Table S1) upper values of G_{sto} were higher about 20% and achieved level of 130 mmol O_3 m^{-2} s^{-1} in maxima.

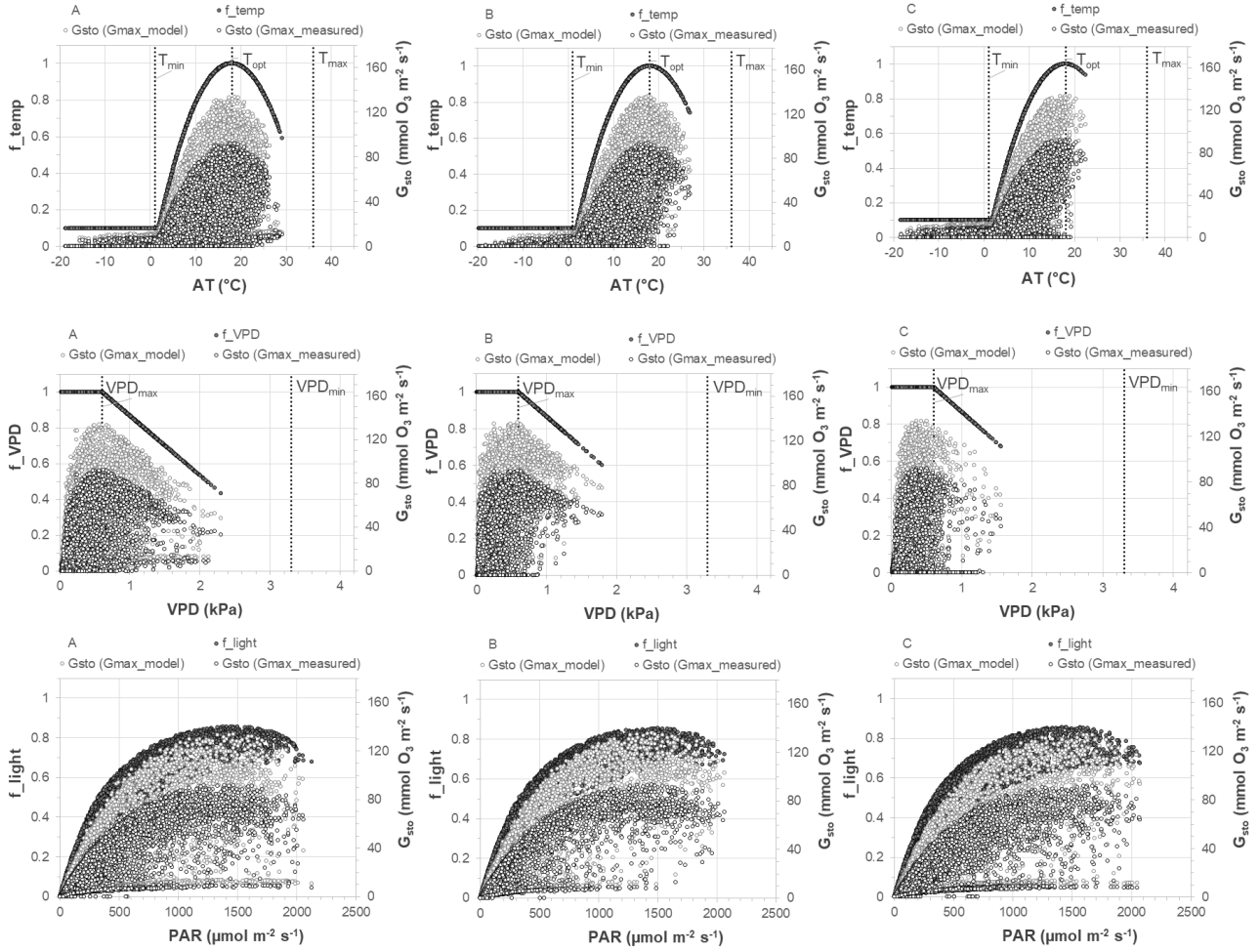

Figure 4. Air temperature (AT, degC), vapour pressure deficit (VPD, kPa), and photosynthetically active radiation (PAR, µmol m^{-2} s^{-1}) in relation to environmental factors (f_temp, f_VPD, f_light) and stomatal conductance (G_{sto}) in different altitudes (A, B, C) in 2016; dotted vertical lines depict range of variables (AT, VPD) for effective stomatal O_3 conductance (Table S1).

230 The effect of soil moisture regime on Gsto was analysed according to modelled and measured SWP values and f_SWP function (Eq. 7). Differences between SWP values modelled via DO_3SE and SWP measured in submontane (B) and subalpine zone (C) were negligible with respect to effective interval SWP_{min} and SWP_{max} (Fig. 5). Factor f_SWP at the level of 1 (i.e. SWP > SWP_max = –0.76 MPa) confirm the assumption that soil moisture at higher altitudes is sufficient for unlimited stomatal conductance and O_3 uptake. However, at the foothill site (A) differences between modelled and measured SWP as well as f_{SWP}

235 were larger. During warm months (May – August) model results and measurement values of SWP decreased to different minimal level of -2.0 MPa and -1.3 MPa, respectively. In addition, measurement of SPW indicates soil water drought events ($SWP < SWP_{max}$) also in autumn (Sep – Oct) and winter (Jan) season while model values varied around level of -0.1 MPa for these periods. It appears that the model generates results inconsistent with measurement of SWP for foothill area (A).

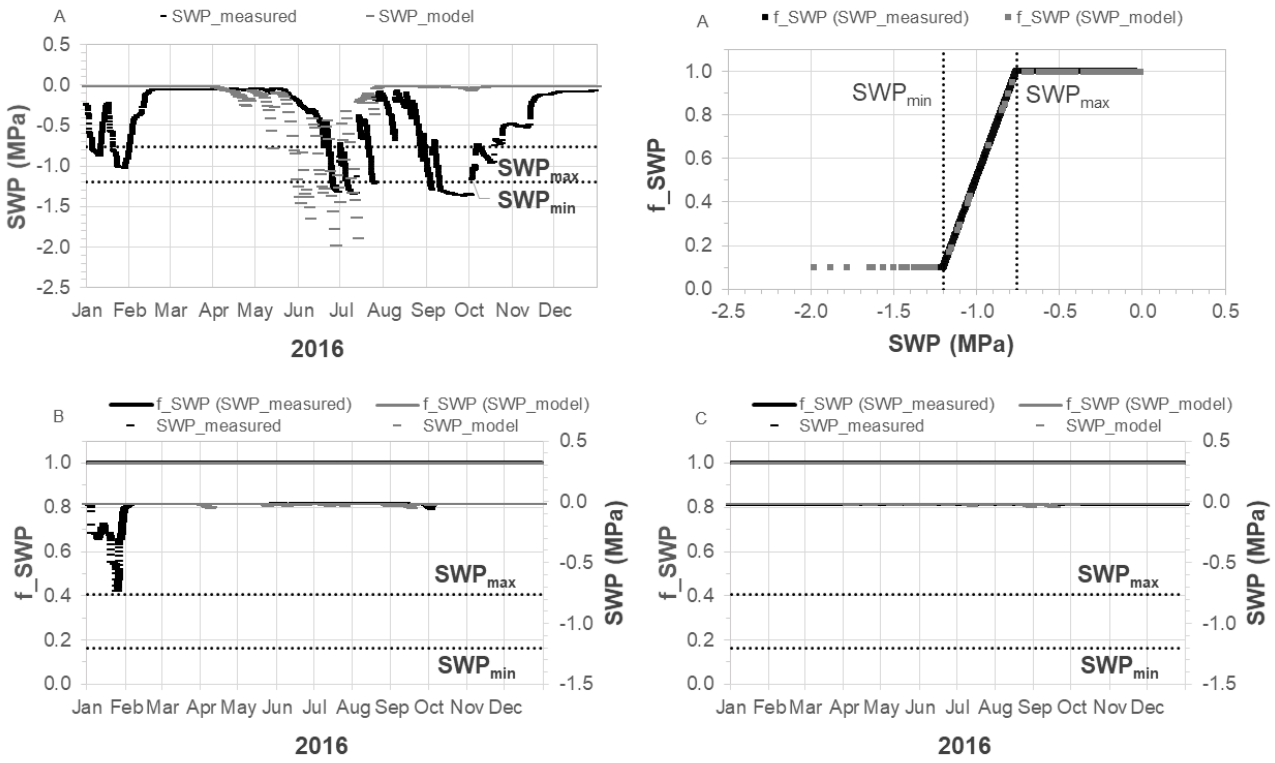

Figure 5. Soil water potential (SWP, MPa) and factor f_SWP (Eq.7): comparison between measured and modelled values for different altitudes (A, B, C) in 2016; dotted lines illustrate range of SWP for effective stomatal O_3 conductance (Table S1).

Stomatal conductance calculated by DO_3SE (Eq. 1) and site-specific model (Eq. 8) were compared at three study sites (A, B and C). In order to archive comparable datasets some data were excluded from the assessment. Due to erroneous instrument response below 5 °C and unreliable measurement below 8 °C (chaotic stomata behaviour) only data with AT above 9 °C were chosen for comparison (cca 3% data size reduction). The second criterion for data reduction (cca 8%) was low PAR. The reason was slow stomata response to PAR below 150 umol on one side and fast change of VPD on the other. On average, stomata adaptation to changing light conditions in gasometer chamber lasted almost 40 minutes. Thus to keep other environmental parameters constant in field conditions was almost impossible. It should be stated here that according to gasometric measurement PAR above 150 umol did not noticeably control stomatal conductance and this is also a reason why PAR did not appear in site-specific model. Stomatal conductance for O_3 uptake by dwarf mountain pine estimated by DO_3SE and site-specific model at three study sites is shown in Fig. 6. The average values of stomatal conductance estimated by two models were rather similar at all three sites as noted in Fig. 6. On all sites differences in temporal variation were more pronounced. Generally stomatal conductance interpreted with DO_3SE was more flattened than presented the site-specific model.

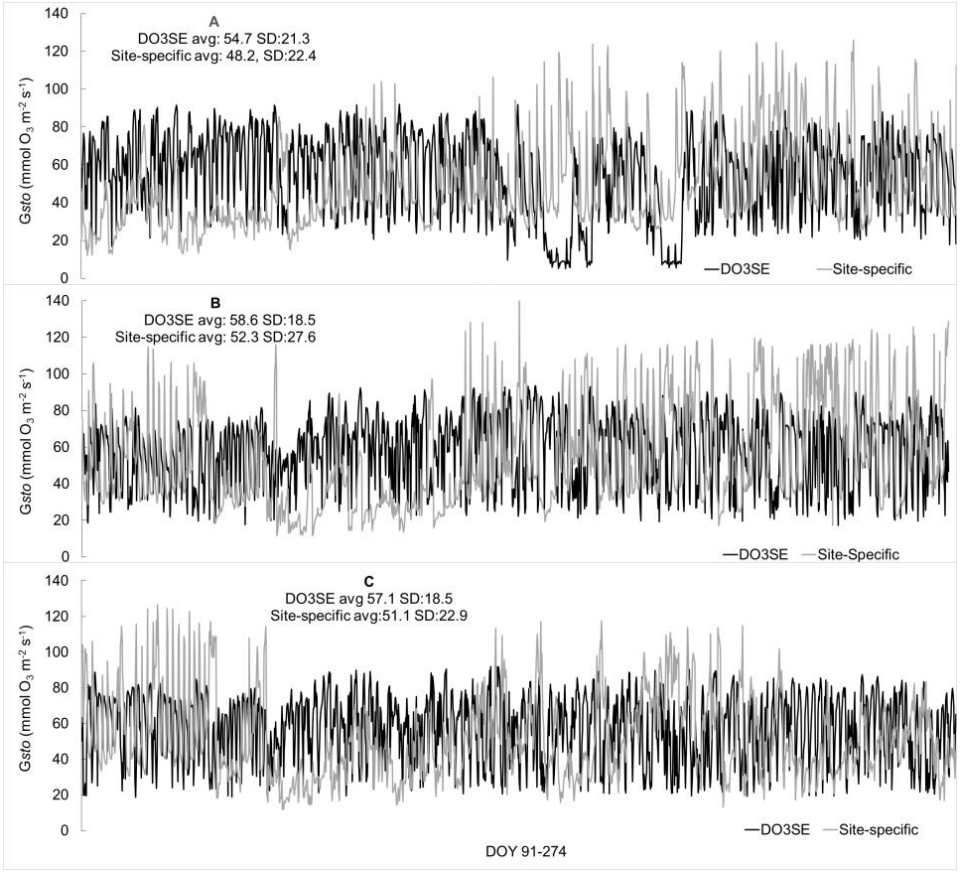

Figure 6. Stomatal conductance G_{sto} (mmol O_3 m^{-2} s^{-1}) according to DO_3SE (Eq.1) and site-specific model (Eq. 8) estimated for selected meteorological conditions (AT above 9 °C and PAR above 150 umol m^{-2} s^{-1} from April 1st till September 30th DOY 91–274) for dwarf mountain pine at three study sites (A, B, C) in SK–HT: avg–average G_{sto} and SD–standard deviation.

4.3 Phytotoxic ozone dose and stomatal O_3 uptake

The DO_3SE model results (Table 3) show increase of stomatal O_3 uptake in dwarf mountain pine from foothills (A) to subalpine zone (C) that correspond with a rise of O_3 concentration along altitudinal zones (Fig. 3a). Accumulated stomatal O_3 flux without a threshold (Y=0), POD_0, ranged from 19.1 to 22.1 mmol m^{-2} PLA if we considered environmental factors (R_f_{ENVI}) and maximal stomatal conductance ($M1\_G_{max}$ =110 mmol O_3 m^{-2} s^{-1}) derived from real field measurements. These values are lower about 22–38 % in comparison with POD_0 based on model preset parameter ($M2\_G_{max}$=160 mmol O_3 m^{-2} s^{-1}). Model simulation of environmental factors MS_f_{ENVI} suggests weak growth of POD_Y (up to 5%) in conditions totally unlimited by VPD (f_{VPD}=1), PAR (f_{light}=1), and SWP (f_{SWP}=1) at higher altitudes (B, C). Saturated SWP (f_{SWP}=1) in foothills where soil drought events occurred could move level of POD_Y up by 20% in maxima. The highest increase of POD_Y (30–103%) resulted

from simulation considering optimal air temperature conditions (f_{temp}=1). This simulation suggests the possibility of a further rise of POD_0 in relation to effect of global warming. However, real air temperature were mostly under value of T_{opt}, POD_0 exceeded critical level for highly O_3 sensitive pine conifers (CLef=19 mmol m^{-2} PLA) at all plots (A, B, C). Phytotoxic ozone dose (POD_1) with a threshold Y=1 varied in range from 8.4 to 11.6 mmol m^{-2} PLA. Critical level of POD_1 for dwarf mountain pine has not been determined yet, although an exceedance $CLef_1$ (9.2 mmol m^{-2} PLA) proposed for Norway spruce was noticed just on plots (B, C) representing forest belt between submontane and subalpine zone where dwarf mountain pine naturally occurs.

Table 3. DO_3SE model outputs for POD_1 and POD_0 ozone metrics

CODE site	Y=0 Y=1	POD_Y (mmol m^{-2} PLA) M1: measured G_{max} = 110 mmol O_3 m^{-2} s^{-1} (Fig. 2) f_{ENV} (Eq.1)					POD_Y (mmol m^{-2} PLA) M2: model G_{max} = 160 mmol O_3 m^{-2} s^{-1} (Table S1) f_{ENV} (Eq.1)				
		R_ real	MS_model simulation f_{ENVI}				R_ real	MS_model simulation f_{ENVI}			
		f_{ENVI}	f_{temp}= 1	max_f_{light}	f_{VPD} = 1	f_{SWP} = 1	f_{ENVI}	f_{temp}= 1	max_f_{light}	f_{VPD} = 1	f_{SWP} = 1
A	POD_0	19.1	24.9	20.6	19.6	19.9	23.3	30.2	25.0	23.6	26.4
B	POD_0	19.9	27.9	21.3	20.4	19.9	26.6	37.0	28.6	27.2	26.6
C	POD_0	22.1	38.3	23.0	22.3	22.1	30.6	52.5	31.8	30.8	30.6
A	POD_1	8.4	11.8	9.0	9.1	8.9	12.2	16.9	13.0	12.8	14.6
B	POD_1	10.3	15.0	10.6	10.8	10.3	16.1	23.4	16.9	16.7	16.1
C	POD_1	11.6	23.6	11.8	11.8	11.6	19.2	37.5	19.6	19.3	19.2
	POD_Y ratio			f_{ENVI} (MS : R)			G_{max} (M2 : M1)		f_{ENVI} (MS : R)		
A	POD_0	:	1.30	1.08	1.03	1.04	1.22	1.30	1.07	1.01	1.13
B	POD_0	:	1.40	1.07	1.03	1.00	1.34	1.39	1.08	1.02	1.00
C	POD_0	:	1.73	1.04	1.01	1.00	1.38	1.72	1.04	1.01	1.00
A	POD_1	:	1.40	1.07	1.08	1.06	1.45	1.39	1.07	1.05	1.20
B	POD_1	:	1.46	1.03	1.05	1.00	1.56	1.45	1.05	1.04	1.00
C	POD_1	:	2.03	1.02	1.02	1.00	1.66	1.95	1.02	1.01	1.00

4.4 Visible ozone injury

Dwarf mountain pine branches sampled along the vertical profile from 800 to 2,000 m a.s.l. showed an obvious visible O_3 injury at higher altitudes (Fig. 7). More pronounced visual symptoms were observed for two year old needles (C+2) with percentage of 18.2 ± 2.3 % than one year old needles (C+1) with percentage of 7.7 ± 1.1 %. At all plots, the oldest needles were damaged by O_3 more frequently than the younger ones. The youngest, current year needles did not show any chlorotic mottle or marbling as characteristic markers of O_3 damages. Also we found no differences between southern and northern

exposures. Higher percentage of visible O_3 symptoms could be caused by mild winter of 2015/2016 with unusually low snow cover in SK–HT plots. The dwarf mountain pine which is usually covered by snow in spring was exposed to ambient air O_3 maxima in 2016. Trend lines (Fig. 7) show increase for both POD_0 and percentage of visible O_3 injury in dependency on altitude. This observation confirms that dwarf mountain pine is sensitive to ozone and seems to be an appropriate conifer species for further monitoring of O_3 injury at SK–HT.

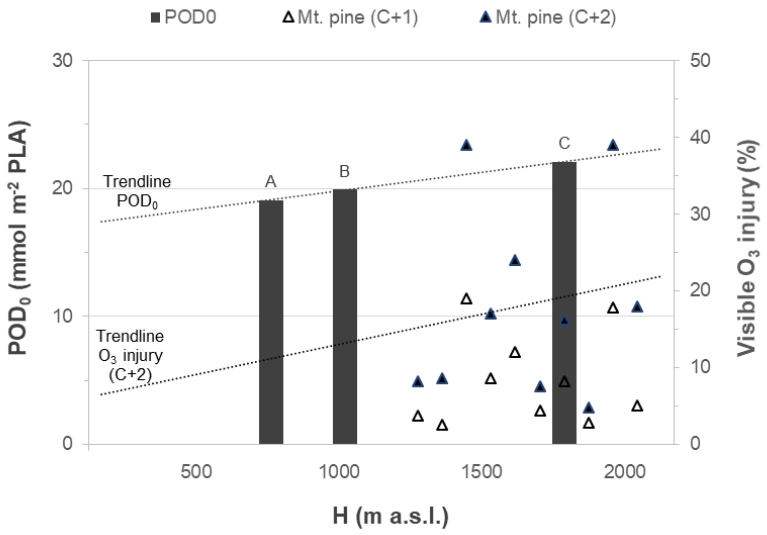

Figure 7. POD_0 in different altitudes (A, B, C) and percentage of visual O_3 symptoms on needles of different age (C+1, C+2) of dwarf mountain pine in SK–HT mountain environment.

5 Discussion

Estimation of phytotoxic effect of ozone on coniferous trees at high elevation and vulnerable mountain forests needs a special approach. Model simulation of stomatal O_3 uptake requires continuous field measurement of hourly O_3 concentration and various meteorological parameters. Precise parameterization of the DO_3SE model is also important for calculation of an accumulated stomatal O_3 flux i.e., POD_Y metrics. Such data is widely available for some commonly occurring trees species, such as Norway spruce (ICP, 2016; Mills et al., 2011) with low sensitivity to O_3 exposures (Coulston et al., 2003). However, there is still a lack of empirical data concerning potentially vulnerable mountain forest tree species. Therefore modification of input parameters reflecting real environment conditions of specific coniferous species may be very useful, especially maximal stomatal conductance of mountain pines.

In this work, we modified maximal stomatal conductance G_{max}=160 mmol O_3 m^{-2} PLA s^{-1} generally used in DO_3SE model as a standard for coniferous tree species. Based on real-time measurements of mountain pines in SK–HT we changed this preset value to the adjusted G_{max}=110 mmol O_3 m^{-2} PLA s^{-1} (Table S1). This modification resulted in POD_Y values substantially lower (22% – 64%) than those predicted by the DO_3SE model with preset G_{max} value. For this reason we recommend to carry

out field measurements of stomatal conductance for determination of correct parameter G_{max} that respects local environmental conditions of selected tree species. Similarly, local parameterization of environmental functions f_{ENVI} including effects of meteorological factors and soil moisture on stomatal conductance G_{sto} (Eq.1) should be useful for verification of DO_3SE model results.

It is necessary to consider some degree of uncertainty of the DO_3SE model in animation of stomata functioning driven mostly by soil water potential. Within our research, the inconsistency between modelled and measured SWP (Fig. 5) for foothills underline the necessity to include site specific real–time SWP data into the DO_3SE model. However e.g. in study (Büker et al., 2015) the experimentally induced soil water stress was not found to substantially reduce PODy, mainly due to the short duration of soil water stress periods. For significant reduction of stomatal conductance and hence O_3 fluxes, more prolonged episodes of reduced water availability are needed. Sufficient amount of precipitation and soil water in submontane and subalpine zones eliminated effect of SWP (Eq. 7, Fig. 5) on stomatal conductance (Eq. 1). This fact caused that function $f_{SWP}=1$ was negligible for the POD_Y calculation (Eq. 2). Mostly cold and humid climate caused that the meteorological factors f_{temp} (Eq. 4, Fig. 5) and f_{VPD} (Eq. 4, Fig. 5) did not reduced O_3 uptake due to absence of very hot and dry weather at higher altitudes. The effect of air temperature on stomatal O_3 conductance tested by model simulation for T_{opt} (Table S1) shows theoretical values of POD larger (30−203%) in comparison with real conditions (Table 3). Although in the near future we cannot expect such steep changes of air temperature in subalpine zone, there is an assumption for rise of O_3 uptake associated with global warming. According to data collected at meteorological observatory Skalnaté Pleso, annual average air temperature fluctuated around the long-term average for the 1941−1991 period of 1.8 °C. The average annual temperature was already 3.1 °C during 2004−2015 and reached maximum values of ~4 °C at the end of this period (Kopáček et al., 2017).

Beside these findings our study revealed the importance of the night-time plant transpiration and stomatal conductance for more precise estimation of POD_o values. The DO_3SE model sets the night-time values to zero and thus underestimate stomatal conductance during night. Our preliminary night-time physiological measurements on dwarf mountain pine (unpublished data) indicate the role of night time fluxes similarly as in other tree species (Zeppel et al., 2013).

The study Büker et al. (2015) showed that it is possible to define dose–response relationships both by species as well as by plant functional types and that the use of a simplified parameterisation of the stomatal conductance model can provide reasonable accuracy in the calculation of PODy for non-Mediterranean tree species. Our study supports good performance of DO_3SE model in specific local conditions concerning stomatal conductance G_{sto}. We confirmed reliable estimation of G_{sto} by direct gasometric measurements (Fig. 6) and developed site-specific stomata response function (Eq. 8). Differences between the two models on three study sites were below 12%. On the other hand, temporal variation showed notable differences. Contrary to relatively flattened DO_3SE, stomatal conductance by site-specific model was notably more sensitive to environmental variables. At this stage we cannot conclude if divergence in model predictions would yield different POD especially in coniferous species with less evident phenology.

Based on the outputs of our study we can confirm that visible O_3 injury increases with rising altitude (Díaz-de-Quijano et al., 2009; Kefauver et al., 2014). A fact that O_3 concentrations and O_3 uptake into the foliar tissues rise with altitude is supported

by many previous studies (Chevalier et al., 2004; Bičárová et al., 2013). Relatively high percentage of visible O_3 injury observed on *P. mugo* may be related to specific micro-site conditions of growth (Coulston et al., 2003; Nunn et al., 2007; Braun et al., 2014). Recently method used for evaluation of O_3 injury symptoms on conifers may produce some questionable results as discussed by several authors (e.g. Wieser et al., 2006), however, it is the only easily detectable evidence of ozone injury in the field. Ozone induced visible injury comes about as a result of oxidative stress, leaves no elemental residues detected by analytical techniques. In combination with the measurement of O_3 concentrations and the modelling of O_3 uptake, the assessment of O_3 visible injury can be valuable tool to estimate the potential risk for European ecosystems (ICP, 2017). Within our study, the dose-response relationship was proved in Fig. 7 showing both trend lines of the ozone visible injury and POD_0 values as well. Obvious visual symptoms associated with high O_3 uptake of dwarf mountain pine show high potential risk of O_3 pollution for subalpine ecosystems in SK–HT. Dwarf mountain pine should be subject of further research activities focused on biomonitoring of O_3 injury in mountain environment.

6 Conclusions

The present paper deals with the phytotoxic ozone effect on dwarf mountain pine occurring in the highest part of the Carpathian mountain forests. Dwarf mountain pine is a typical tree species of the timberline area exposed to high ambient O_3 concentration. The assessment of adverse O_3 response on mountain conifer was based on measurement of O_3 concentration in combination with modelling of O_3 uptake and observation of O_3 induced visible injury. Our results confirmed expected increase of O_3 concentrations as well as O_3 uptake and phytotoxic ozone dose (POD) with increasing altitudes. Model values of POD_0 exceeded critical level for high O_3 sensitive pine tree species on all three experimental plots where field measurement of O_3 concentration and meteorological data processed in model were carried out during year round period of 2016. Environmental factors reflecting air humidity and soil moisture conditions almost unlimited capture of O_3 in tissues of conifer needles in area between submontane and subalpine zone. In foothills, we noticed reduction of O_3 uptake as response to the serious soil moisture deficit in the summer season. However, validation of modelled against measured values of soil water potential (SWP) show inconsistency and then for modelling of the stomatal O_3 flux is important to take into account field measurement of SWP, especially in areas where soil drought events occur. The effect of air temperature on stomatal O_3 conductance corresponds with relatively cold climate in High Tatra Mts. Model simulation considering optimal air temperature conditions suggests higher O_3 uptake associated with global warming. According to field measurement, we modified key parameter i.e. maximal stomatal conductance G_{max} for local environmental conditions. This modification resulted in POD_0 values substantially lower (22–66%) than those predicted by the DO_3SE model with preset G_{max} generally used as a standard for coniferous tree species. Field observations of O_3 induced visible injury on dwarf mountain pine confirmed that older needles were more damaged by O_3 than the younger ones. Incidence of visible O_3 symptoms is consistent with measurement of O_3 concentration and modelled values of POD metrics. Obtained results suggest further risk for ecological services provided by dwarf pine in sensitive High Tatra Mts environment.

Team list

Author contribution: S. Bičárová, H. Pavlendová, Z. Sitková designed and carried field measurement of O_3, meteorological variables and SWP; S. Bičárová calculated O_3 metrics; H. Pavlendová assessed visual O_3 injury and Z. Sitková analysed SWP data; P. Fleischer jr. and P. Fleischer sr. designed and carried field measurement of stomatal conductance for dwarf mountain pine; A. Bytnerowicz suggested methodological improvements of field experiments and helped with preparing and writing of the manuscript. All authors discussed the results and contributed to the final manuscript.

Competing interests: The authors declare that they have no conflict of interest.

Supplement Part SI–1: Details in section Methods: DO_3SE model parameterization (Table S1)

Acknowledgements
This work was supported by the Slovak Research and Development Agency under the contracts No. APVV–0429–12, APVV–16–0325, and by the Grant Agency of the Slovak Republic (VEGA, No.2/0053/14 and No. 2/0026/16). We acknowledge also the project ITMS 26220220066 funded by ERDF (10 %). The authors are grateful to the Slovak Hydrometeorological Institute (SHMI) for providing of meteorological, climatic and EMEP data. The development of DO_3SE model interface has been made possible through funding provided by the UK Department of Environment, Food and Rural Affairs (Defra) and through institutional support provided to the Stockholm Environment Institute from the Swedish International Development Agency (Sida).

References

1. Ashmore, M., Emberson, L., Karlsson, P. E., and Pleijel, H.: New Directions: A new generation of ozone critical levels for the protection of vegetation in Europe. Atmos. Environ., 38, 2213–2214, http://doi.org/10.1016/j.atmosenv.2004.02.029, 2004.
2. Bičárová, S., Pavlendová, H., and Fleischer, P.: Vulnerability to ozone air pollution in different landforms of Europe. In Sethi R (ed) Air pollution: Sources, prevention and health effects, Nova Science Publishers, New York, 25–63. 2013.
3. Bičárová, S., Sitková, Z., and Pavlendová, H.: Ozone phytotoxicity in the Western Carpathian Mountains in Slovakia, Lesnícky časopis - Forestry Journal, 62, 77–88, 2016.
4. Braun, S., Schindler, C., and Rihm, B.: Growth losses in Swiss forests caused by ozone: Epidemiological data analysis of stem increment of Fagus sylvatica L. and Picea abies Karst, Environ. Pollut., 192, 129–138, http://doi.org/10.1016/j.envpol.2014.05.016, 2014.
5. Büker, P., Feng, Z., Uddling, J., Briolat, A., Alonso, R., Braun, S., Elvira, S., Gerosa, G., Karlsson P. E., Le Thiec, D., Marzuoli, R., Mills, G., Oksanen E., Wieser, G., Wilkinson, M., and Emberson, L. D.: New flux based dose-response relationships for ozone for European forest tree species. Environ. Pollut., 206, 163–174. 2015
6. Büker, P., Morrissey, T., Briolat, A., Falk, R., Simpson, D., Tuovinen, J.-P., Alonso, R., Barth, S., Baumgarten, M., Grulke, N., Karlsson, P. E., King, J., Lagergren, F., Matyssek, R., Nunn, A., Ogaya, R., Peñuelas, J., Rhea, L., Schaub, M., Uddling, J., Werner, W., and Emberson, L. D.: DO3SE modelling of soil moisture to determine ozone flux to forest trees, Atmos. Chem. Phys., 12, 5537–5562, doi:10.5194/acp-12-5537-2012, 2012.
7. Bussotti, F., Desotgiu, R., Cascio, C., Pollastrini, M., Gravano, E., Gerosa, G., Marzuoli, R., Nali, C., Lorenzini, G., Salvatori, E., Manes, F., Schaub, M., and Strasser, R. J.: Ozone stress in woody plants assessed with chlorophyll a fluorescence. A critical reassessment of existing data, Environ. Exp. Bot., 73, 19–30, http://doi.org/10.1016/j.envexpbot.2010.10.022, 2011.
8. Bytnerowicz, A., Godzik, B., Grodzińska, K., Frączek, W., Musselman, R., Manning, W., Badea, O., Popescu, F., and Fleischer, P.: Ambient ozone in forests of the Central and Eastern European mountains, Environ. Pollut., 130, 5–16, http://doi.org/10.1016/j.envpol.2003.10.032, 2004.
9. CLRTAP: Mapping Critical Levels for Vegetation, Chapter III of Manual on methodologies and criteria for modelling and mapping critical loads and levels and air pollution effects, risks and trends. UNECE Convention on Long range Transboundary Air Pollution www.icpmapping.org, 2015.
10. CLRTAP: Mapping Critical Levels for Vegetation, Chapter III of Manual on methodologies and criteria for modelling and mapping critical loads and levels and air pollution effects, risks and trends. UNECE Convention on Long range Transboundary Air Pollution www.icpmapping.org, 2017.
11. Cooper, O. R., Parrish, D. D., Ziemke, J., Balashov, N. V., Cupeiro, M., Galbally, I. E., and … Zbinden, R. M.: Global distribution and trends of tropospheric ozone: An observation-based review, Elem. Sci. Anth, 2, 29, http://doi.org/10.12952/journal.elementa.000029, 2014.
12. Coulston, J. W., Smith, G. C., and Smith, W. D.: Regional Assessment of Ozone Sensitive Tree Species Using Bioindicator Plants, Environ. Monit. Assess., 83, 113–127, http://doi.org/10.1023/A:1022578506736, 2003.

13. Dalstein, L., and Vas, N.: Ozone Concentrations and Ozone-Induced Symptoms On Coastal and Alpine Mediterranean Pines in Southern France, Water Air Soil Poll., 160, 181–195, http://doi.org/10.1007/s11270-005-4144-7, 2005.

14. De Marco, A., Sicard, P., Vitale, M., Carriero, G., Renou, C., and Paoletti, E.: Metrics of ozone risk assessment for Southern European forests: Canopy moisture content as a potential plant response indicator, Atmos. Environ., 120, 182–190, http://doi.org/10.1016/j.atmosenv.2015.08.071, 2015.

15. Díaz-de-Quijano, M., Peñuelas, J., and Ribas, À.: Increasing interannual and altitudinal ozone mixing ratios in the Catalan Pyrenees, Atmos. Environ., 43, 6049–6057, http://doi.org/10.1016/j.atmosenv.2009.08.035, 2009.

16. Dizengremel, P., Jolivet, Y., Tuzet, A., Ranieri, A., and Le Thiec, D.: Integrative Phytotoxic Ozone Dose Assessment in Leaves in View of Risk Modelling for Forest Ecosystems. In: R. Matyssek, N. Clarke, P. Cudlin, T. N. Mikkelsen, J.-P. Tuovinen G. Wieser, & E. Paoletti (Eds.), Climate Change, Air Pollution and Global Challenges: Knowledge, Understanding and Perspectives from Forest Research, Elsevier Physical Sciences Series "Developments in Environmental Science" 13, 267–283, 2013.

17. Dole-Olivier, M.-J., Galassi, D. M. P., Fiers, F., Malard, F., Martin, P., Martin, D., and Marmonier, P.: Biodiversity in mountain groundwater : The Mercantour National Park (France) as a European hotspot Biodiversity in mountain groundwater : the Mercantour National Park (France) as a European hotspot, Zoosystema, 37, 529–550, doi:10.5252/z2015n4A, 2015.

18. EEA: Report No 28/2016: Air quality in Europe. : http://www.eea.europa.eu/publications/air-quality-in-europe-2016, 2016.

19. Emberson, L. D., Ashmore, M. R., Cambridge, H. M., Simpson, D., and Tuovinen, J. P.: Modelling stomatal ozone flux across Europe, Environ. Pollut., 109, 403–413, http://doi.org/10.1016/S0269-7491(00)00043-9, 2000.

20. Emberson, L. D., Büker, P., Ashmore, M. R. : Assessing the risk caused by ground level ozone to European forest trees: A case study in pine, beech and oak across different climate regions. Environ. Pollut., 147, 454–466. DOI: 10.1016/j.envpol.2006.10.026, 2007.

21. EPA: Health Risk and Exposure Assessment for Ozone https://www3.epa.gov/ttn/naaqs/standards/ozone/data/20140829healthrea.pdf, 2014.

22. Feng, Z. Z., Büker, P., Pleijel, H., Emberson, L. D., Karlsson, P.E., Uddling, J. : A unifying explanation for variation in ozone sensitivity among woody plants. Global Change Biology, 24, 1–7, https://doi.org/10.1111/gcb.13824promoting, 2017.

23. Fleischer, P., Pichler, V., Fleischer Jr, P., Holko, L., Máliš, F., Gömöryová, E., Cudlín, P., Holeksa, J., Michalová, Z., Homolová, Z., Skvarenina, J., Střelcová, K., Hlaváč, P.: Forest ecosystem services affected by natural disturbances, climate and land-use changes in the Tatra Mountains, Climate Research, 73/1, 1–15. DOI:10.3354/cr01461, 2017.

24. Fuhrer, J., Skärby, L., and Ashmore, M. R.: Critical levels for ozone effects on vegetation in Europe, Environ. Pollut., 97, 91–106, http://doi.org/10.1016/S0269-7491(97)00067-5, 1997.

25. Gottardini, E., Cristofori, A., Cristofolini, F., Nali, C., Pellegrini, E., Bussotti, F., and Ferretti, M.: Chlorophyll-related indicators are linked to visible ozone symptoms: Evidence from a field study on native Viburnum lantana L. plants in northern Italy, Ecological Indicators, 39, 65-74, http://doi.org/10.1016/j.ecolind.2013.11.021, 2014.

26. Grünhage, L., Krause, G. H. M., Köllner, B., Bender, J., Weigel, H. J., Jäger, H . J., and Guderian, R.: A new flux-orientated concept to derive critical levels for ozone to protect vegetation, Environ. Pollut., 111, 355–362, http://doi.org/10.1016/S0269-7491(00)00181-0, 2001.

27. Hůnová, I., Novotný, R., Uhlířová, H., Vráblík, T., Horálek, J., Lomský, B., and Šrámek, V.: The impact of ambient ozone on mountain spruce forests in the Czech Republic as indicated by malondialdehyde, Environ. Pollut., 158, 2393–2401, http://doi.org/10.1016/j.envpol.2010.04.006, 2010.

28. ICP: ICP Vegetation, Chapter 3, Mapping critical levels for vegetation: http://icpvegetation.ceh.ac.uk/publications/documents/Chapter3-Mappingcriticallevelsforvegetation_000.pdf, 2016.

29. ICP: ICP FORESTS 2016 Executive report: https://icp-forests.org/pdf/ER2016.pdf, 2017.

30. Karlsson, P. E., Braun, S., Broadmeadow, M., Elvira, S., Emberson, L., Gimeno, B. S., Le Thiec, D., Novak, K., Oksanen, E., Schaub, M., Uddling, J., and Wilkinson, M.: Risk assessments for forest trees: The performance of the ozone flux versus the AOT concepts, Environ. Pollut., 146, 608–616, http://doi.org/10.1016/j.envpol.2006.06.012, 2007.

31. Kefauver, S. C., Pe, J., Ribas, A., Díaz-de-quijano, M., and Ustin, S.: Using Pinus uncinata to monitor tropospheric ozone in the Pyrenees, Ecol. Indic., 36, 262–271. http://doi.org/10.1016/j.ecolind.2013.07.024, 2014.

32. Kopáček, J., Kaňa, J., Bičárová, S., Fernandez, I .J., Hejzlar, J., Kahounová, M., Norton, S. A., Stuchlík, E.: Climate change increasing calcium and magnesium leaching from granitic Alpine catchments, Environ. Sci. Technol., 51/1, 159-166, DOI: 10.1021/acs.est.6b03575, 2017

33. Krupa, S. V., and Legge, A. H.: Passive sampling of ambient, gaseous air pollutants: an assessment from an ecological perspective, Environ. Pollut., 107, 31–45, http://doi.org/10.1016/S0269-7491(99)00154-2, 2000.

34. Lefohn, A. S., Malley, C. S., Simon, H., Wells, B., Xu, X., Zhang, L., and Wang, T.: Responses of human health and vegetation exposure metrics to changes in ozone concentration distributions in the European Union, United States, and China, Atmos. Environ., 152, 123–145, http://doi.org/10.1016/j.atmosenv.2016.12.025, 2017.

35. Loibl, W., Smidt, S.: Ozone exposure – Areas of potential ozone risks for selected tree species. Environ. Sci. Pollut. Res. 3, 213–217, https://doi.org/10.1007/BF02986962, 1996.

36. Loibl, W., Winiwarter, W., Kopsca, A., Zueger, J., and Baumann, R.: Estimating the spatial distribution of ozone concentrations in complex terrain. Atmos. Environ. 28, 2557–2566, https://doi.org/10.1016/1352-2310(94)90430-8, 1994.

37. Massman, W. J., Musselman, R. C., and Lefohn, A. S.: A conceptual ozone dose-response model to develop a standard to protect vegetation, Atmos. Environ., 34, 745–759, http://doi.org/10.1016/S1352-2310(99)00395-7, 2000.

38. Massman, W. J.: A review of the molecular diffusivities of H2O, CO2, CH4, CO, O3, SO2, NH3, N2O, NO, and NO2 in air, O2 and N2 near STP, Atmos. Environ., 32, 1111–1127, http://doi.org/10.1016/S1352-2310(97)00391-9, 1998.

39. Matyssek, R., Bytnerowicz, A., Karlsson, P. E., Paoletti, E., Sanz, M., Schaub, M., and Wieser, G.: Promoting the O3 flux concept for European forest trees, Environ. Pollut., 146, 587–607, http://doi.org/10.1016/j.envpol.2006.11.011, 2007.

40. Mezei, P., Jakuš, R., Pennerstorfer, J., Havašová, M., Škvarenina, J., Ferenčík, J., Slivinský, J., Bičárová, S., Bilčík, D., Blaženec, M., Netherer, S.: Storms, temperature maxima and the Eurasian spruce bark beetle Ips typographus—An infernal trio in Norway spruce forests of the Central European High Tatra Mountains. Agr. Forest Meteorol., 242, 85–95, doi:10.1016/j.agrformet.2017.04.004, 2017.

41. Mills, G., Pleijel, H., Braun, S., Büker, P., Bermejo, V., Calvo, E., Danielsson, H., Emberson, L., Fernández, I. G., Grünhage, L., Harmens, H., Hayes, F., Karlsson, P.-E., and Simpson, D.: New stomatal flux-based critical levels for ozone effects on vegetation, Atmos. Environ., 45, 5064–5068, http://doi.org/10.1016/j.atmosenv.2011.06.009, 2011.

42. Mills, G., Harmens, H., Wagg, S., Sharps, K., Hayes, F., Fowler, D., Sutton, M., and Davies, B.: Ozone impacts on vegetation in a nitrogen enriched and changing climate, Environ. Pollut., 208, Part B, 898–908, http://doi.org/10.1016/j.envpol.2015.09.038, 2016.

43. Musselman, R. C., Lefohn, A. S., Massman, W. J., and Heath, R. L.: A critical review and analysis of the use of exposure- and flux-based ozone indices for predicting vegetation effects, Atmos. Environ., 40, 1869–1888, http://doi.org/10.1016/j.atmosenv.2005.10.064, 2006.

44. Nunn, A. J., Wieser, G., Metzger, U., Löw, M., Wipfler, P., Häberle, K.-H., and Matyssek, R.: Exemplifying whole-plant ozone uptake in adult forest trees of contrasting species and site conditions, Environ. Pollut., 146, 629–639, http://doi.org/10.1016/j.envpol.2006.06.015, 2007.

45. Paoletti, E., and Manning, W. J.: Toward a biologically significant and usable standard for ozone that will also protect plants, Environ. Pollut., 150, 85–95, http://doi.org/10.1016/j.envpol.2007.06.037, 2007.

46. SEI: DO_3SE (Deposition of ozone for stomatal exchange) https://www.sei-international.org/do3se, 2014.

47. Sicard, P., Dalstein-Richier, L., and Vas, N.: Annual and seasonal trends of ambient ozone concentration and its impact on forest vegetation in Mercantour National Park (South-eastern France) over the 2000–2008 period, Environ. Pollut., 159, 351–362, http://doi.org/10.1016/j.envpol.2010.10.027, 2011.

48. Sicard, P., De Marco, A., Dalstein-Richier, L., Tagliaferro, F., Renou, C., and Paoletti, E.: An epidemiological assessment of stomatal ozone flux-based critical levels for visible ozone injury in Southern European forests, Sci. Total Environ., 541, 729–741, http://doi.org/10.1016/j.scitotenv.2015.09.113, 2016.

49. Smidt, S., and Herman, F.: Evaluation of air pollution-related risks for Austrian mountain forests, Environ. Pollut., 130, 99–112, http://doi.org/10.1016/j.envpol.2003.10.027, 2004.

50. UNECE: Towards Cleaner Air Scientific Assessment Report 2016: http://www.unece.org/index.php?id=42861, 2016.

51. Vollenweider, P., and Günthardt-Goerg, M. S.: Erratum to "Diagnosis of abiotic and biotic stress factors using the visible symptoms in foliage" [Environ. Pollut. 137 (2005) 455–465], Environ. Pollut., 140, 562–571, http://doi.org/10.1016/j.envpol.2006.01.002, 2006.

52. Wagner, S., Kronberger, G., Beham, A., Kommenda, M., Scheibenpflug, A., Pitzer, E.,Vonolfen, S., Kofler, M., Winkler, S., Dorfer, V., Affenzeller, M.: Architecture and Design of the HeuristicLab Optimization Environment, In Advanced Methods and Applications in Computational Intelligence, Topics in Intelligent Engineering and Informatics Series, Springer, pp. 197–261. https://doi.org/10.1007/978-3-319-01436-4_10, 2014.

53. WHO: Air Quality Guidelines. Global Update 2005. Particulate matter. ozone. nitrogen dioxide and sulfur dioxide. http://www.euro.who.int/__data/assets/pdf_file/0005/78638/E90038.pdf, 2006.

54. Wieser, G., Manning, W. J., Tausz, M., and Bytnerowicz, A. : Evidence for potential impacts of ozone on Pinus cembra L. at mountain sites in Europe: An overview. Environ. Pollut., 139, 53–58. doi:10.1016/j.envpol.2005.04.037, 2006.

55. Zapletal, M., Pretel, J., Chroust, P., Cudlín, P., Edwards-Jonášová, M., Urban, O., Pokorný, R., Czerný, R., and Hůnová, I.: The influence of climate change on stomatal ozone flux to a mountain Norway spruce forest, Environ. Pollut., 169, 267–273, http://doi.org/10.1016/j.envpol.2012.05.008, 2012.

56. Zeppel, M., Logan, B.A., Lewis, J.D., Phillips, N., and Tissue, D.T.: Nocturnal sap flow and stomatal conductance: a review, Conference paper, 2013.